

Effect of tribofilm derived from phosphorus/sulfur additives on pitting resistance of bearing steel during rolling friction

Yunah Jeung*, Ryotaro Ohashi**, Ryosuke Kitamura**, Kaisei Sato*, Shinya Sasaki*

*Tokyo University of Science, **Graduate school of Tokyo University of Science

1. Introduction

Electric vehicles (EVs) are increasingly being promoted as environmentally friendly transportation options that play a vital role in addressing issues such as global warming and air pollution. With advancements in technology leading to improvements in driving distance and charging time of EVs, the adoption of EVs is rapidly increasing in various types of automobiles. Consequently, there is a growing focus on the development of lubricants that can enhance the power efficiency of automobiles.

To achieve improvement of fuel/power efficiency of automobiles, lubricants have gradually proceeded to become lower viscosity. Lowering the viscosity reduces viscous drag, thus enhancing the fuel/power efficiency. However, lower viscosity leads to a thinner lubricating film, increasing the direct contacts between two sliding substrates and consequently causing issues such as scuffing and seizure etc. Therefore, it is necessary to enhance the reliability of low-viscosity lubricants by employing lubricant additives. Commonly used lubricant additives include phosphorus-based and sulfur-based additives. phosphorus-based additives primarily function to mitigate wear by adsorbing and reacting on the sliding surface to form a reaction film and prevent wear. Sulfur-based additives are utilized as extreme pressure additives that can prevent seizure by forming a reaction film between solid surfaces. However, it has been reported that the use of lubricant additives can lead to increase fatigue wear under rolling conditions (reference). Furthermore, the precise mechanisms of surface protection by phosphorus-based and sulfur-based additives during rolling contact have not been fully elucidated.

Purpose of this study is to investigate the surface damage mechanism of lubricants containing phosphorus-based and sulfur-based additives. Using an MTM traction tester, fatigue tests under rolling-sliding conditions were conducted with lubricants containing phosphorus-based and sulfur-based additives. The performance of the additives was compared, and the structures of the reaction films were analyzed by X-ray photoelectron spectroscopy (XPS), a nano-indenter and focused ion beam–scanning transmission electron microscopy (FIB-STEM).

2. Experiment

2.1 Lubricants

Table 1 shows the base lubricant and additives used for rolling friction fatigue tests. Poly-alpha-olefin 4 (PAO4) served as base oil, while Alkylamine salts of phosphoric acid esters and sulfurized olefins were utilized as the phosphorus-based (P-based additive) and sulfur-based additives (S-based additive), respectively. The concentration of each additive was maintained at 0.08 P mass% for phosphorus-based additives and 0.17 S mass% for S-based additives. Three types of lubricants were prepared: lubricant with singular addition of phosphorus-based additives to base oil, lubricant with singular addition of S-based additives to the base lubricant, and lubricant with a combination use of phosphorus-based and S-based additives (P/S-based additive) added to the base lubricant.

Table 1 Lubricants used in our experiments

Lubricant	Additive
PAO4	-
P-based	Alkylamine salts of phosphoric acid esters
S-based	Sulfurized Olefin
P/S-based	Alkylamine salts of phosphoric acid esters Sulfurized Olefin

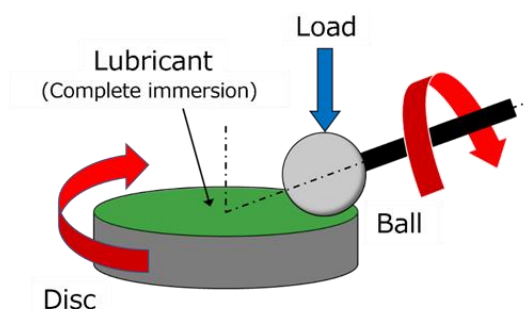


Fig. 1 Configuration of rolling friction fatigue tests

2.2 Rolling friction fatigue test

For rolling friction fatigue tests, we used ball-on-disk type-traction tester (MTM2, PCS Instruments, UK). Figure 1 shows the test configuration, while Table 2 shows the detailed specifications of the test samples. Both disk and ball used were SUJ2 in our experiments. On the evaluation of the fatigue damage ratio and wear amount, we investigated ball side specimen. Additionally, to facilitate the occurrence of micro-pitting, the arithmetic mean surface roughness Ra of the disk was ground to 0.3 - 0.4 μm . Table 3 shows the test conditions for the Rolling friction Fatigue Tests.

Table 2 Specimen specifications

	Ball	Disc
Material	SUJ2	
Hardness, HV	800 ~ 920	720 ~ 780
Surface roughness, μm	~ 0.02	0.3 ~ 0.4

Table 3 Test conditions

Lubricant temperature, $^{\circ}\text{C}$	65
Load, N	75
Entrainment speed, mm/s	3000
Slide-roll-ratio (SRR), %	0, 5
Lubricant volume, mL	50
Test time, h	48
Number of cycles	9 million

2.3 Surface observation

Following the rolling friction fatigue test, surface morphologies were analyzed by a confocal laser microscope (VK-X150, KEYENCE, JP) and an optical microscope (KEYENCE VHX-8000, Keyence, Japan). To quantitatively evaluate the area percentage of fatigue wear, binarization was performed as a threshold of the maximum wear depth after Rolling friction Fatigue Tests for each test specimen. Furthermore, to determine the damaged area percentage (DAP) ¹⁾, surface images of the wear track were acquired and analyzed at eight locations on each ball.

2.4 Tribofilm analysis & surface hardness

We also performed composition analysis and evaluated surface hardness of the reaction films formed by each lubricant. These investigations were carried out using an XPS (Axis nova, Shimadzu, Japan) and a nano-indenter (iMicro, Nanomechanics, US). XPS analysis examined the composition of the reaction films acquiring the peaks corresponding to P 2p and S 2p on the worn surface of each ball. Furthermore, for the S-based additives, XPS depth profiling of the reaction film was conducted by Ar etching. In the nano-indentation measurements, the hardness of the reaction film at a depth of 20 nm was investigated using the Berkovich tip. Furthermore, to investigate the structure of the reaction film, cross-sectional images were acquired using FIB-STEM.

3. Results

3.1 Rolling friction fatigue test

Figure 2 shows the results of surface images of damage on the ball after rolling friction fatigue tests. At SRR 0%, for PAO4, it was confirmed that significant wear and micro-pitting occurred. Next, for P-based additive, indentation, wear scar and micro-pitting were observed on the wear track, and it is considered that fatigue and abrasive wear occurred, respectively. Additionally, for the S-based additive, no significant wear were observed compared to the P-based additive, but micro-pitting occurred on the sliding surface. Finally, for the P/S-based additive, indentation and micro-pitting observed in P-based and S-based additives were confirmed. The trend observed at SRR5% was similar to that at SRR0%.

Figures 3 and 4 show the results of wear volume and DAP. Comparing SRR0% with SRR5%, it was found that wear volume and DAP at SRR0% were smaller than those at SRR5%. Moreover, significant differences in wear volume and DAP were observed depending on the additive types. For PAO4 at SRR5%, the wear volume was $6.1 \times 10^3 \mu\text{m}^3$, indicating the highest wear volume. Comparing each lubricant, the wear volumes for P-added lubricant, S-added lubricant and P/S-added lubricant were $4.2 \times 10^3 \mu\text{m}^3$, $2.9 \times 10^3 \mu\text{m}^3$ and $2.7 \times 10^3 \mu\text{m}^3$. In these lubricants, P-added lubricant indicated the highest wear volume, followed by the S-based additive, and the P/S-based additive. Regarding DAP, P-added and P/S-added lubricants were 1.10% and 1.14%, respectively. The DAP included abrasive wear, micro-pitting, and indentation, therefore, in P-added and P/S-added lubricants, DAP increased for the reason that abrasive wear, micro-pitting, and indentation occurred overall. On the other hand, for PAO4, it was 0.6%, indicating a relatively smaller DAP, which is believed that wear remove the surface of the micro-pitting and indentation because the wear volume of P-added and P/S-added lubricants showed the higher than that of S-added lubricant.

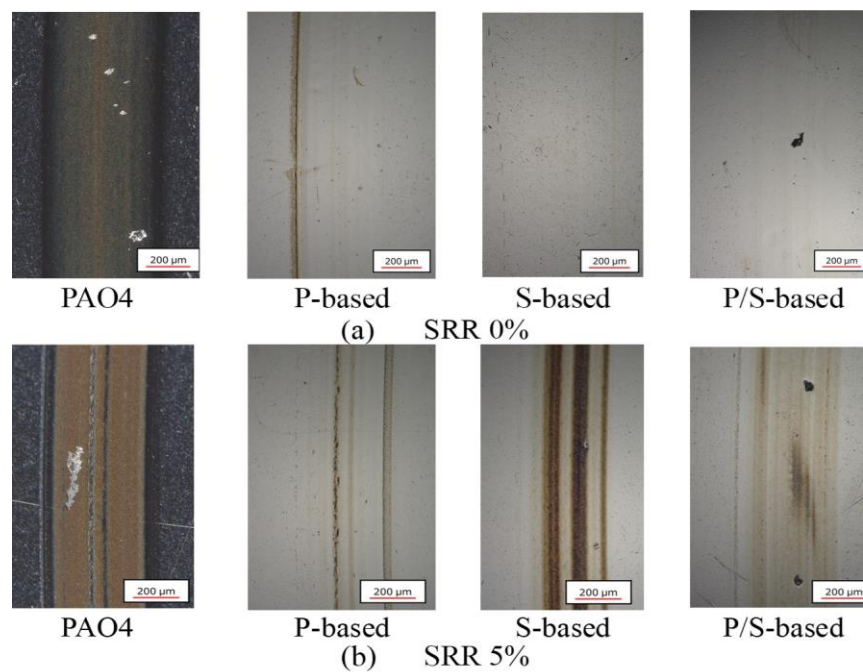


Fig. 2 Surface image of ball specimens observed by digital microscope and depth of damages after the test

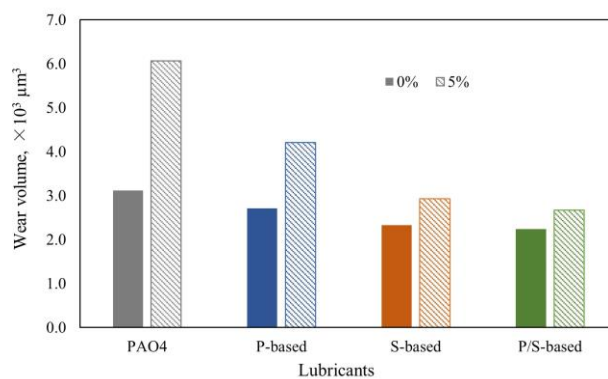


Fig. 3 Wear volume

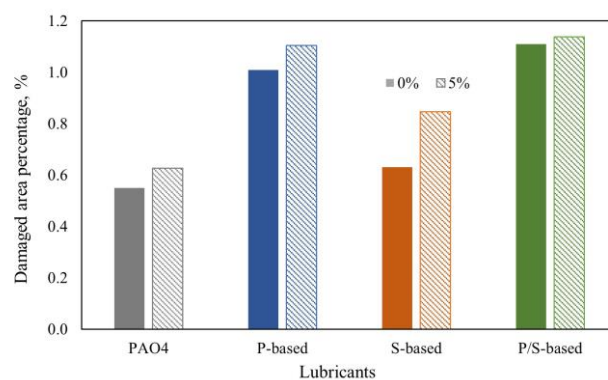


Fig. 4 Damaged Area Percentage (DAP).

3.2 Tribofilm analysis & Surface hardness

Figure 5 shows the results of XPS analysis of the surfaces after rolling friction fatigue tests using each lubricant. From Fig. 5, P-derived and S-derived peaks were observed on the wear track of P-added and S-added lubricant, respectively. On the wear track of P/S-added lubricant, both peaks derived from P and S were observed. From these elemental peaks, the formation of tribofilms was found. Additionally, based on the binding energy of each peak, iron phosphate in P-added lubricant, iron sulfate in the S-added lubricant, and both iron phosphate and iron sulfate in P/S-added lubricant were generated. Figure 6 shows the results of XPS depth profiling of S-added lubricant. From Fig. 6, iron sulfate and sulfide were detected after zero and five seconds of Ar etching, respectively.

Figure 7 shows cross-sectional images of wear tracks observed via FIB-STEM for each lubricant. Upon examination of Fig. 7, it is evident that a tribofilm of approximately 100 nm thickness was formed with the P-based additive. Additionally, both S-added and P/S-added lubricants formed significantly thicker tribofilms, measuring 200 nm, in comparison to those formed with the P-based additives. Notably, the tribofilm generated in S-added lubricant displayed stratified structure, aligning with the findings of XPS depth profiling.

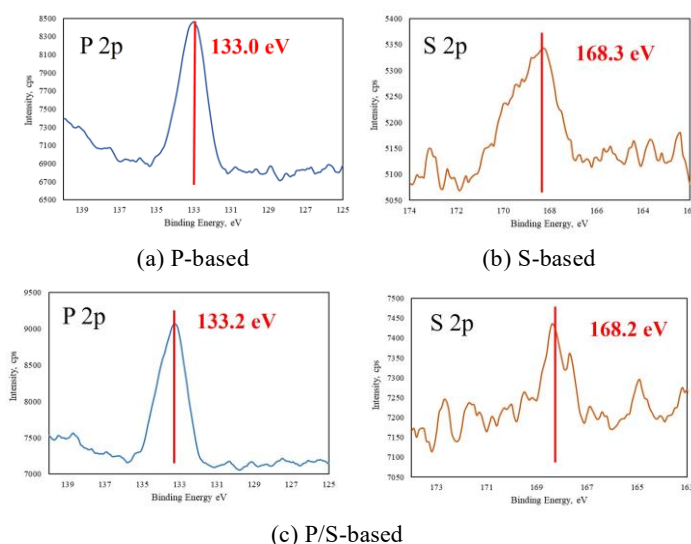


Fig. 5 XPS peaks of wear tracks measured using each lubricant (SRR 0%).

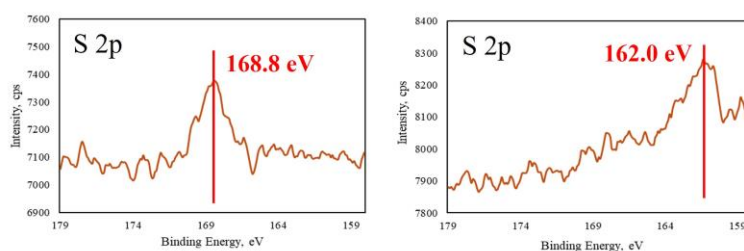


Fig. 6 XPS peaks of S-based additives (SRR 0%) before and after Ar etching

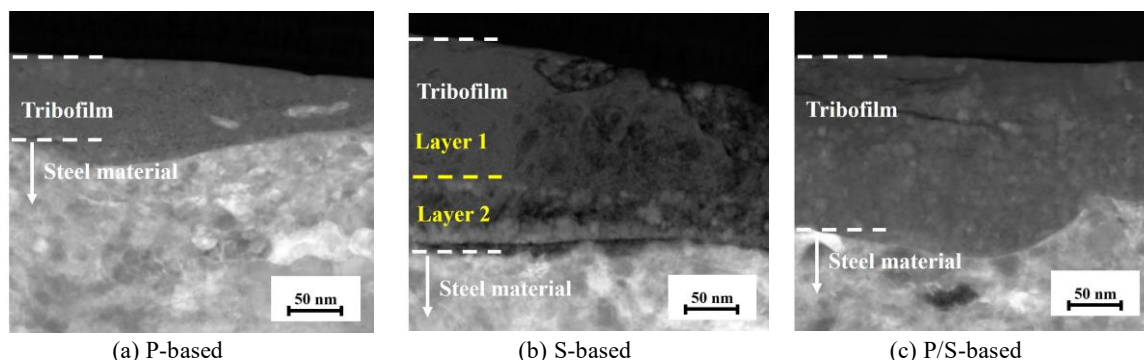


Fig. 7 Cross-sectional images of tribofilm observed by FIB-STEM

Figure 8 shows the results of nano-indentation measurements. In the nano-indentation tests, S-based additives exhibited higher surface hardness compared to P-based additives under all sliding conditions. Moreover, the hardness of P/S-based additive increased with the increase of SRR and the trend was confirmed in the case of S-based additive.

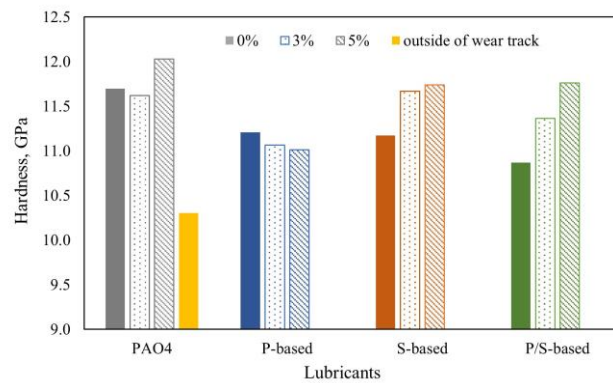


Fig. 8 Surface hardness using a nano-indenter

4. Discussion

4.1 Changes of chemical composition of tribofilm formed by P/S-based additive by sliding

Table 4 shows the composition ratio of the tribofilm formed by P-based, S-based and P/S-based lubricants. It is evident that in both P-based and S-based additive's tribofilm, the concentrations of P and S increased due to sliding. Furthermore, the ratio of S concentration to P concentration in P/S-based additive's tribofilm was found to be 6.08% and 9.60% from SRR0% and SRR5%, respectively, indicating an increase in S concentration ratio due to sliding. Therefore, it is believed that sliding promotes the tribofilm growth of S-based additives. Focusing on the change in surface hardness, it is observed that the surface becomes harder in case of S-based and P/S-based upon sliding occurrence. Thus, regardless of the coexistence of P-based additive, S-based additive significantly increased surface hardness by forming a S-rich film due to sliding.

Table 4 The changes in the concentration of each element when used individually and when used in combination

Element		P, %	S, %
SRR 0%	P-based	1.64	-
	S-based	-	0.32
	P/S-based	2.16	0.14
SRR 5%	P-based	3.67	-
	S-based	-	0.39
	P/S-based	2.73	0.29

4.2 Investigation of tribofilm structure in S-based additives

Figure 9 shows the tribofilm model based on the results of XPS depth profiling (Fig. 6). In the case of S-added lubricant, it is assumed to exhibit a dual-layer tribofilm consisting of iron sulfate and an iron sulfide. Furthermore, dual-layer tribofilm were confirmed in cross-sectional images obtained through FIB-STEM analysis (Fig. 7). Generally, S-based additive is known to form soft tribofilm, which make it possible to disturb seizure by sacrificing themselves due to being soft. However, we confirmed that S-based tribofilm was hard based on the results of a nano-indenter. We considered that this discrepancy was caused by the dual-layer tribofilm. Iron sulfate is generally estimated as soft layers because iron sulfate lead to corrosion, but the iron sulfate is quite thin and S-based tribofilm mainly composed of iron sulfide. It is hypothesized that the presence of hard iron sulfide, which has high melting point, contributes to increase surface hardness and reduce wear volume.

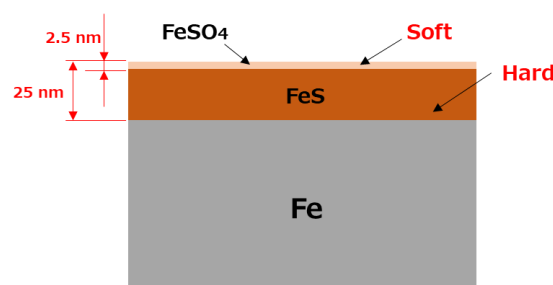


Fig. 9 Tribofilm model formed by S-based additive based on the results of XPS depth profiling

4.3 Correlation between surface hardness, wear volume, and damage area percentage (DAP)

Figure 10 shows the correlation between wear volume and surface hardness after rolling friction fatigue tests with each additive. Comparing different additives at SRR0%, no significant differences in wear volume by increasing hardness were observed. However, upon the occurrence of sliding, S-based and P/S-based additives exhibit a substantial increase in hardness and consequently demonstrate lower wear volumes compared to P-based additives. Hence, it is inferred that the harder surface prevents wear. However, in the case of PAO4, despite its hardness, the wear volume remains high values because PAO4 did not form tribofilm.

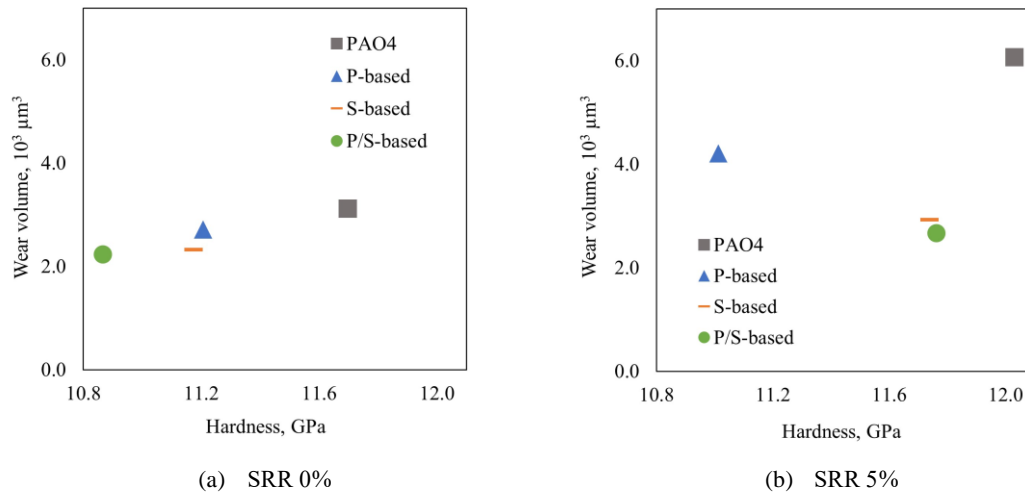


Fig. 10 Correlation between wear volume and surface hardness after fatigue tests

Furthermore, Figure 11 shows the correlation between DAP and surface hardness after fatigue tests with each additive. For SRR0% and SRR5%, it was observed that DAP decreases with increasing hardness. Therefore, it is inferred that DAP is significantly influenced by hardness regardless of the presence of additives. However, in the case of P/S-based additives, despite the increase in hardness due to sliding, they exhibit high DAP. This is believed to be attributed to the presence of P-based.

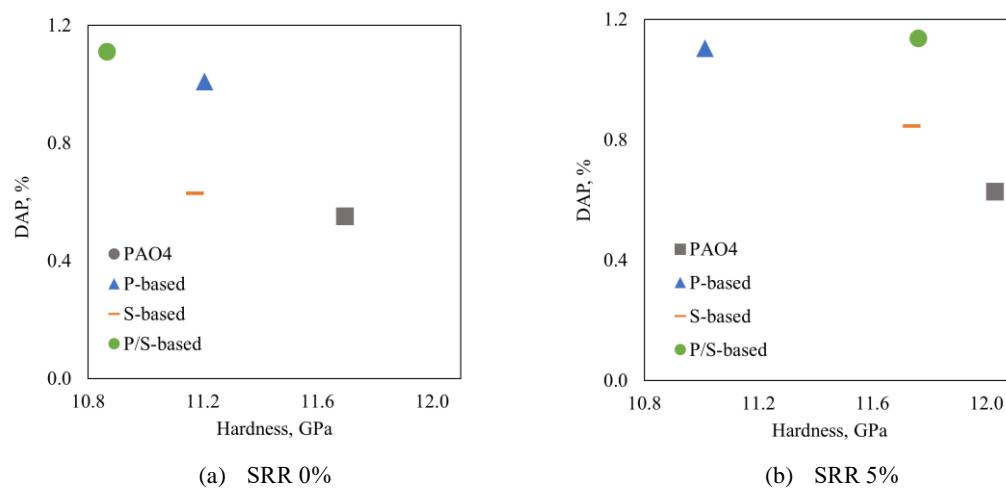


Fig. 11 correlation between DAP and surface hardness after fatigue tests

4.4 Mechanism of wear resistance and pitting resistance in P-based and S-based additives

Figure 12 shows the mechanism of wear resistance and pitting resistance characteristics of each additive. In the case of S-based additive, it is confirmed that hard film is formed. Therefore, it is considered that the hard tribofilm suppresses surface wear. However, the reduction in wear attributed to the absence of removing fatigue surfaces by sliding, leading to the occurrence of micro-pitting associated with fatigue wear. In the case of P-based additive, it formed soft layer, making it more prone to abrasive wear and indentation damage, increasing DAP and wear. In the case of P/S-based additives, mixed tribofilm of P-based and S-based additives were generated and it is considered that P-based and S-based tribofilm have different roles in surface protection. By the influence of the tribofilm's hardness, P-based only tribofilm led to increase DAP and S-based only tribofilm attribute to decrease wear volume (Figures 3 and 4). Based on these results, in P/S-based lubricant, the formation of P-based tribofilm led to the escalation in surface damage ratio, in addition, the incorporation of S-based tribofilm demonstrated the superior anti-wear properties.

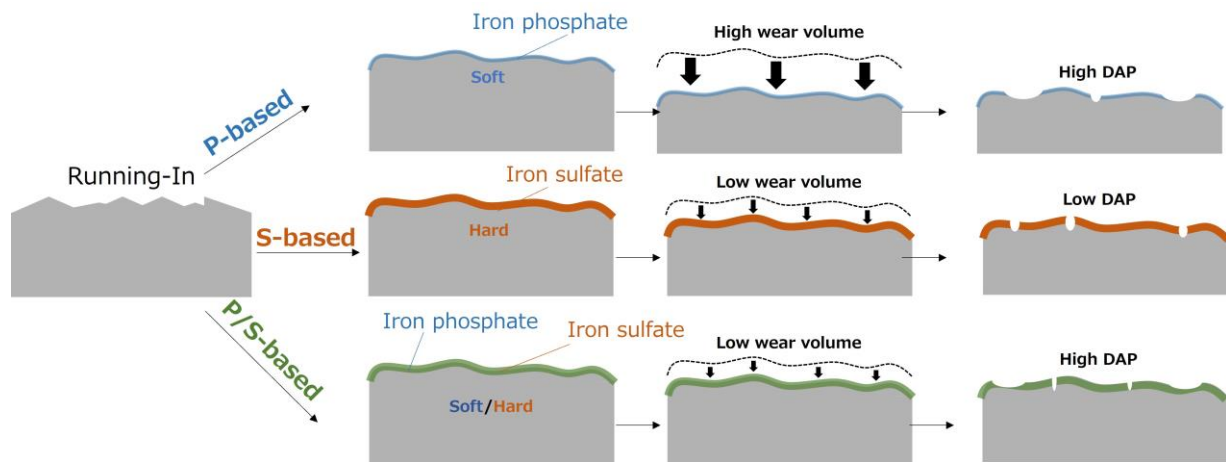


Fig. 12 Mechanism of wear resistance and pitting resistance characteristics of each additive

5. Conclusion

To investigate the surface damage mechanism of lubricants containing phosphorus-based and sulfur-based additives, we conducted evaluations of the wear resistance and pitting resistance of P-based and S-based additives under rolling-sliding conditions, and analyzed the structures and hardness of the reaction films using XPS, a nano-indenter and FIB-TEM. The following conclusions were obtained:

- 1) From the rolling friction fatigue tests, S-based additive exhibited a decrease in wear volume and a lower surface damage percentage compared to P-based additive. This is believed to be attributed to the formation of a hard surface by S-based additive.
- 2) In the rolling friction fatigue tests, the combination of S-based and P-based additives showed the most superior wear resistance. However, DAP was comparable to that of P-based additive alone, resulting in inferior performance compared to S-based additive alone.
- 3) XPS analysis revealed an increase in the concentration of P and S in the tribofilm due to sliding. Particularly, in the case of P/S-based additives, S ratio in tribofilm formation increased, leading to an increase in surface hardness.
- 4) XPS depth profiling and FIB-STEM observations revealed that S-based additive formed two-layered tribofilm consisting of iron sulfate at outermost surface and iron sulfide under iron sulfate. It is believed that this tribofilm structure influenced the decrease in wear volume and surface damage percentage.

References

- 1) Vrcek, A., Hultqvist, T., Johannesson, T., Björling, M., Marklund, P., Larsson, R., Micro-pitting and wear characterization for different rolling bearing steels: Effect of hardness and heat treatments, *Wear*, Vol. 458–459, (2020), pp. 1-10.